MODELING AND MEASUREMENT SYSTEM FOR MAGNETIC FIELD DISTRIBUTIONS IN BIOLOGICAL STRUCTURES

I. Marinova, V. Mateev, H. Endo[*] and Y. Saito[**]
Department of Electrical Apparatus
Technical University of Sofia
Sofia 1756, Bulgraria
Emails: iliana@tu-sofia.bg, vmateev@tu-sofia.bg
[*]Power & Industrial Systems R & D Lab., Hitachi Ltd, Japan
Email: hisashi.endo.fa@hitachi.com
[**] Graduate School of Hosei University, Tokyo 184-8584 Japan
Email: ysaito@hosei.ac.jp

Abstract- In this paper we develop a system for modeling and measurement of magnetic field distributions in biological structures caused by the externally applied electromagnetic field. We describe an effective and versatile approach for three-dimensional reconstruction of the field distributions from two-dimensional visualization the measured magnetic field data. The finite element model for magnetic field calculation is built. The magnetic fields of very thin slices of the 3D object are determined and visualized. Using these 2D images as slices of 3D image and based on the field theory and image processing techniques we developed a reconstruction approach for 3D visualization of magnetic field. This approach combines new technologies of 3D visualizations and characterizes with flexibility, simplicity and portability. The proposed approach was successfully applied for 3D reconstruction and visualization of magnetic field and current distributions in biological structures. The virtual microscope is developed for investigations of magnetic field distributions in biological structures during magnetic stimulation. Anisotropic Magneto-Resistive (AMR) sensors are applied for magnetic field measurements. AMR sensors are combined in array probes in order to increase productivity of measurement process and improving the performance of probes.

Index terms*: Magnetic field modeling, Finite element method, Image reconstruction, Magnetic field, Visualization., AMR sensors array, Magnetic field measurement.

I. INTRODUCTION

In many applications such as nondestructive testing, electromagnetic compatibility, identifications, medical diagnosis and etc., we search for sources or anomalies inside an inaccessible regions. This problem classically is done by detection, localization and characterization. The present development of the measurement devices does well in the detection and localization, but the exact determination of the shape, surface and volume reconstruction of the object under consideration are still a problem of paramount importance. Determination of the field distributions from locally measurements outside the source area formulates the inverse electromagnetic problem. The present visualizing devices, high technology methodologies for visualization, image processing and data manipulations give possibilities for precise analysis and solutions of forward and inverse problems in electromagnetics, medicine, architecture etc. Recently, the field theory and image processing techniques were successfully applied for visualization of electromagnetic fields as well as to several inverse electromagnetic problems [1-3].

In this paper we develop a system for modeling and measurement of magnetic field distribution in biological structures caused by the externally applied electromagnetic field. We propose an approach for 3D field reconstruction visualizing the measured data of 2D magnetic field distributions. The finite element method (FEM) is applied for determination of magnetic field distribution in very thin slices of human leg exposed to externally applied time varying magnetic field. The images obtained by visualizing the magnetic field distributions are considered as slices of 3D image. Based on the field theory and image processing techniques, we built 3D reconstruction approach for 3D visualization of magnetic field. The proposed approach was successfully applied for 3D reconstruction and visualization of magnetic field and current distributions. This approach suggests a possibility for 3D visualization of magnetic field with complex structure and characteristics.

During modeling, simulation and measurements usually very large multidimensional datasets are generated and utilized. In order to facilitate the analysis of the phenomena, processes as well as magnetic field distribution in biological structures during magnetic stimulation the virtual biomagnetic microscope is developed.

The Anisotropic Magneto-Resistive (AMR) sensors are applied for magnetic field measurements [15-21]. AMR sensors are based on anisotropic magnetoresistance effect: the resistivity of ferromagnetic alloys measured in a direction parallel to the magnetization of permalloy film is slightly higher than the resistivity measured perpendicular to the magnetization. The main advantages of AMR sensors compared to Hall sensors are:

- high sensitivity;
- higher accuracy;
- no piezo effect;
- higher operational temperatures.

AMR sensors are combined in array probes in order to increase productivity of measurement process and improving the performance of probes applied for magnetic field measurements in space around coils. The AMR magnetic sensors and sensor arrays offer improvements in speed and resolution in eddy-current testing and bio-magnetic imaging. Arrays of AMR magnetic sensors allow rapid scanning of an area of interest in a single pass. The small size and low power consumption of these solid-state magnetic sensors enable the fabrication of compact arrays of sensors on circuit boards and even on-chip sensor arrays.

II. MAGNETIC FIELD IN HUMAN BODY

The externally applied time-varying magnetic fields are widely used in medicine, especially for diagnosis and therapy. A wide range of frequencies and magnetic field intensities are employed, and various requirements are associated with these applications [4-8]. Applying magnetic field to human body results in current flow and electrical field induced in non-homogeneous and anisotropic biological structures. Magnetic stimulation has become an important powerful tool in neurophysiology. In magnetic stimulation, short and very intensive current pulses are supplied to the coil in order to produce a fast rising, strong magnetic field and to stimulate nerve fibbers in the cerebral cortex or in peripheral nerves [9-13]. Faraday's law expresses the electric field **E** induced in the tissue during externally applied time varying magnetic field .

$$\nabla \times \mathbf{E} = -\frac{\partial \mathbf{B}}{\partial t} \tag{1}$$

where **B** is the magnetic field produced by magnetic stimulation coil with current I and

determined by the Biot-Savart law

$$\mathbf{B} = \frac{\mu_0}{4\pi} I(t) \int_S \frac{\mathbf{dl}(\mathbf{r}') \times (\mathbf{r} - \mathbf{r}')}{|\mathbf{r} - \mathbf{r}'|^3}, \tag{2}$$

where μ_0 is the permeability of free space.

The electric field is expressed by magnetic vector potential **A** and electric potential V as

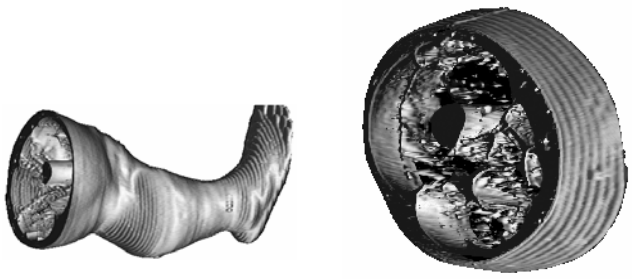
$$\mathbf{E} = -\frac{\partial A}{\partial t} - \nabla V. \tag{3}$$

The magnetic field distribution changes according to respective configuration of electromagnetic systems used to excite the magnetic field in human body.

Development of computation model of magnetic field distributions that take into account all properties and characteristics of the biological structures are extremely important in order to realize effective medical diagnosis and therapy. The numerical methods, e.g. finite element method and boundary element method, are powerful tools to investigate the electric and magnetic field distribution produced by electromagnetic devices. Numerical techniques are capable of analysis of various heterogeneous structures of biological bodies exposed to magnetic fields.

III. MAGNETIC STIMULATION OF HUMAN BODY

The human leg has been exposed to magnetic field excited by coil. The cross-section of the human anatomical leg regions under consideration is shown in Fig. 1(a). The images of the slices with distance 1 cm between them are presented in Fig. 2. A three-dimentional stacked image model in Fig. 1(b) is created from the 2-D slices shown in Fig.2.



(a) (b)

Figure 1. Cross section of human leg.

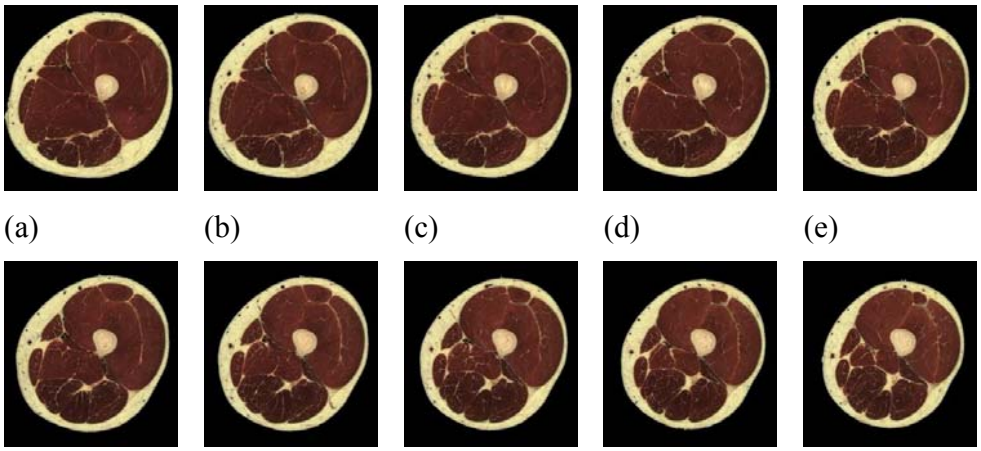


Figure 2. Leg slices at distance 1 cm.

The external magnetic field is excited by standard planar construction of single circular coil for magnetic stimulation with inner diameter - 0.044m and outside diameter - 0.087m. The coil is wound of 9 concentric turns of rectangular copper wire. The magnetic stimulation circular coil is shown in Fig. 3(a). The magnetic field distribution produced by the coil is shown in Fig. 3b.

IV. FINITE ELEMENT MODEL

Three-dimensional finite element model for magnetic field calculations in biological structures is built and applied to the each slice of the human legs shown in Fig. 2.

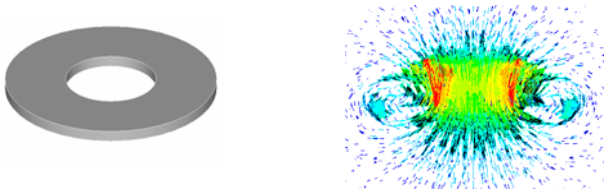


Figure 3. Magnetic stimulation coil and field distribution

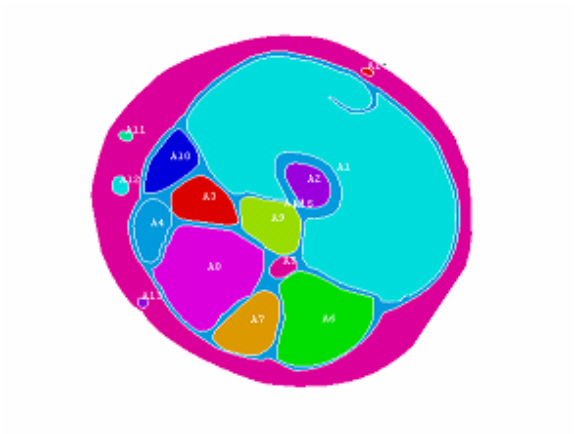


Figure 4. Finite element model areas

Table 1 Tissue properties and model areas

Tissue	Areas	Conductivity σ, S/m
Blood	1,9,11	7.00 e-01
Bone	5	2.03 e-02
Bone marrow	26	8.51 e-01
Fat	24	2.34 e-02
Muscle	2,4,7,8,10,12,15,16,17,18,19	3.34 e-01
Nerve	5	3.20 e-01
White matter	6	6.55 e-02
Skin dermis	25	2.01 e-02

The leg slices are with diameter of 20 cm approximately and length of 1 cm. The slice images are traced and the corresponding areas and volumes for application of FEM are created as shown in Fig. 4. The tissue properties used in the FEM model are listed in Table 1. The medium is accepted to be magnetically homogeneous, with relative magnetic permeability $\mu_r = \mu_0$.

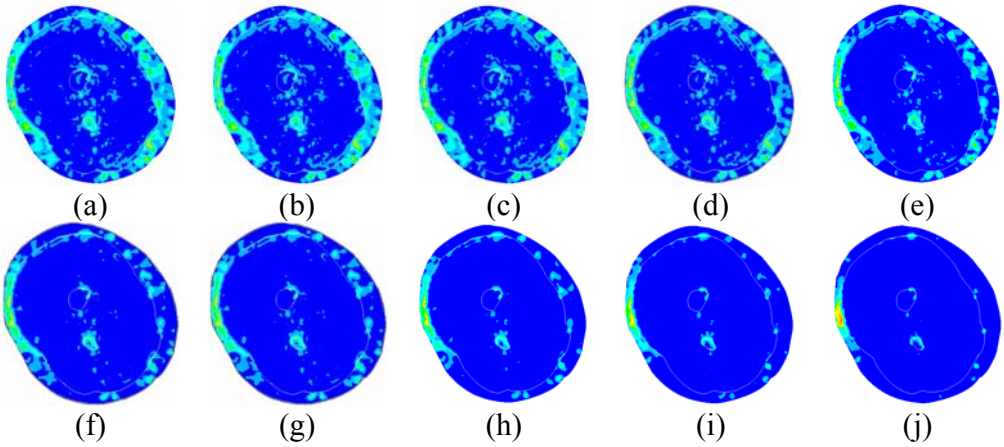


Figure 5. Magnetic field distributions

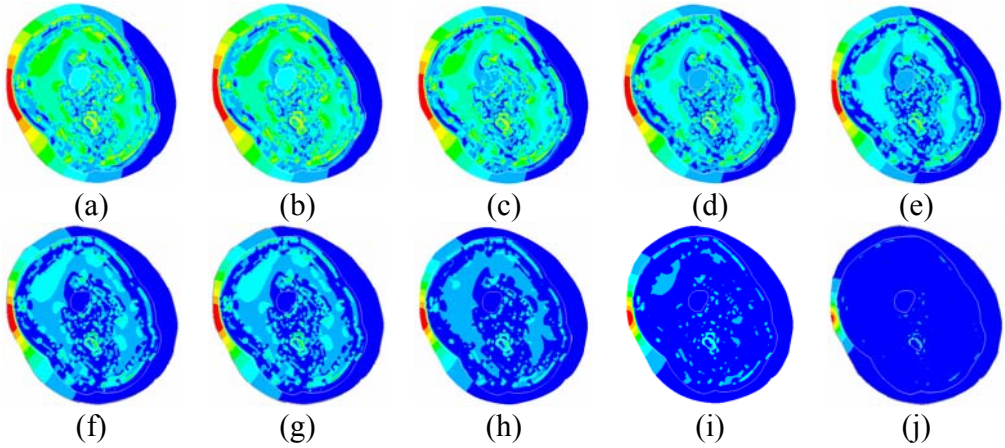


Figure 6. Current distributions

Firstly, the open boundary problem is solved determining the magnetic field distribution of the magnetic stimulation coil for given frequency. As a result, values of the three components of magnetic vector-potential **A** – A_x, A_y, and A_z, at the boundary of the slice under consideration are determined. The relative magnetic homogeneity of biostructures with magnetic permeability $\mu \approx \mu_0$ gives possibility the magnetic vector potential to be determined by expressions

$$\mathbf{A} = \frac{\mu}{\mathbf{4}\pi} \int_V \frac{\mathbf{J}}{\mathbf{r}} dv \,. \tag{4}$$

The components of magnetic vector potential could be considered as independent from the field induced in interior of the region under consideration. This is possible because of the relatively low value of specific conductivity of the biostructures as well as low values of the eddy currents. Secondly, the values of the magnetic vector potential over the slice boundary are imposed as boundary conditions solving the internal Dirichlet boundary problem. As a result the magnetic

field distribution is determined in the slice. Using the developed FEM model the magnetic field was calculated and visualized for each slice of the human leg during magnetic stimulation. The field distribution is investigated at different values of coil current and frequencies. The results presented are for the peak value of the current 1kA with frequency 10 kHz. The magnetic field distributions are visualized and presented in Fig. 5. Figure 6 shows the current distributions caused by the induced voltage.

V. 3D RECONSTRUCTION OF MAGNETIC FIELD

A 3D volume of data for visualization of magnetic field was created from the 2D slices of locally determined and visualized magnetic field distribution at parallel surfaces by transforming each pixel in the 2D slice to its corresponding 3D location using the position, orientation and Green's function. If the 2D slices are arbitrary oriented and positioned in space, some of the voxels in the volume data set are not assigned intensity values. These voxels were identified and assigned an intensity value based on the weighted average of its neighboring voxels. Consequently resembled 3D magnetic field data set is visualized.



(a) Upper part (b) Lower part

Figure 7. 3D reconstruction of magnetic field distributions



(a) Upper part (b) Lower part

Figure 8. 3D reconstruction of current distributions

Combining the 2D magnetic fields shown in Fig. 5 does the 3D reconstruction and visualization of magnetic field. The 3D magnetic field of the human leg under consideration is shown in Fig. 7. Fig. 8 shows the 3D reconstructed current distributions. Thus, using the 2D magnetic field and current distributions the 3D reconstruction is realized.

VI. VIRTUAL BIOMAGNETIC MICROSCOPE

The virtual biomagnetic microscope has been design and implemented for analysis of biomagnetic field distributions [14]. The system store and processes the extremely large quantities of data required to represent a collection of slides as well as provides an access to archived digital slide images. The virtual biomagnetic microscopy is capable to explore the most important characteristics of fields and regions of interest as concentration and localization, zoom, focus-in-depth of magnetic field, etc. The Virtual Microscope is a client-server system designed to provide a realistic digital emulation of a high power light microscope. The architecture of the developed virtual microscope is shown in Fig. 9.

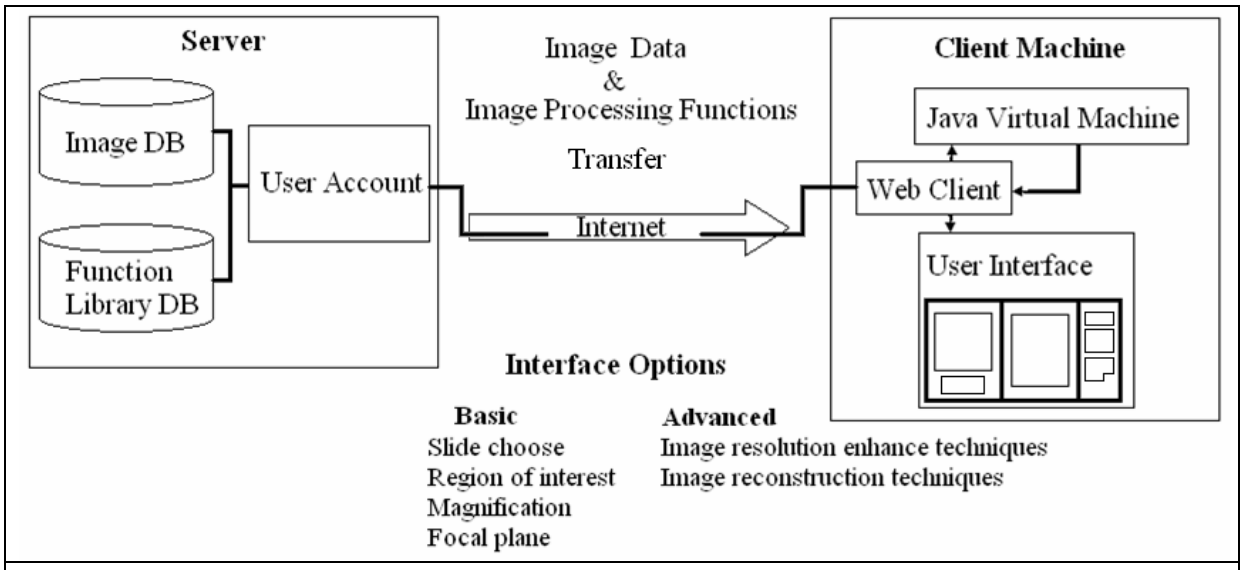


Figure 9 Basic architecture of the virtual microscope

The 3D virtual microscope interface shown in Fig. 11 consists of 3D anatomy display window, the 3D field distribution window and control window. The 3D biological display window shows the 3D reconstruction of the available biological slices of the object under consideration. The 3D Field Distribution window shows the 3D field distribution of the object obtained by reconstruction of 2D field distribution presented by 2D virtual biomagnetic microscope interface shown in Fig. 10.

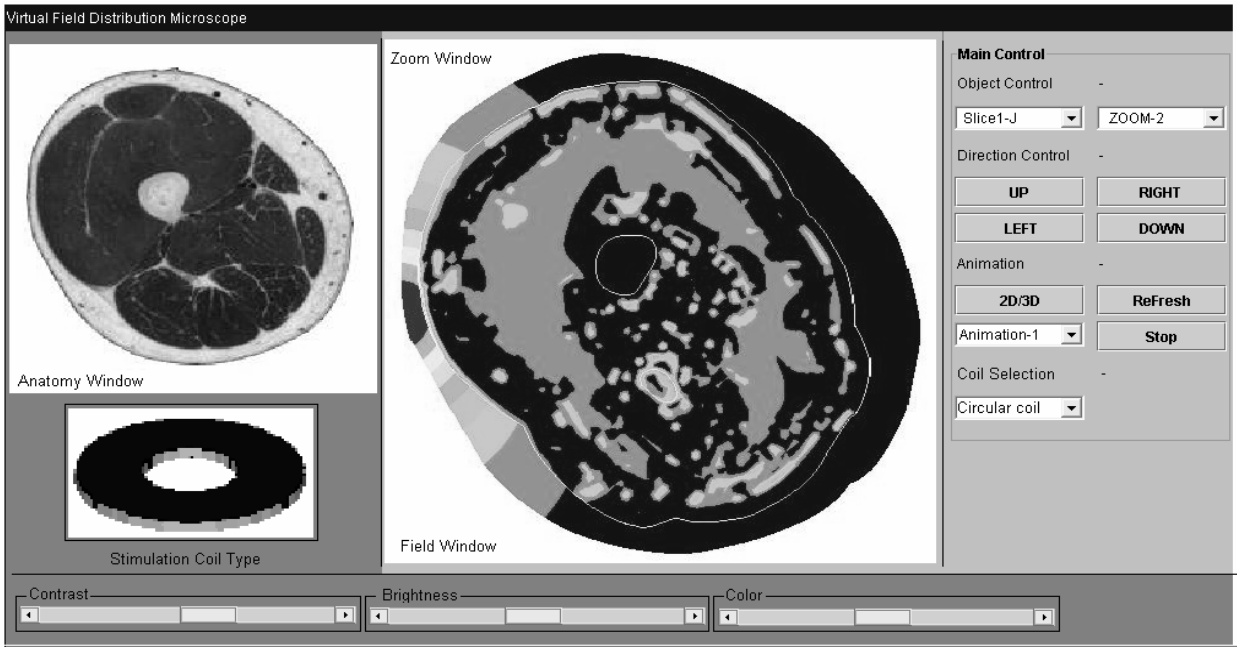


Figure. 10. 2D Virtual microscope interface

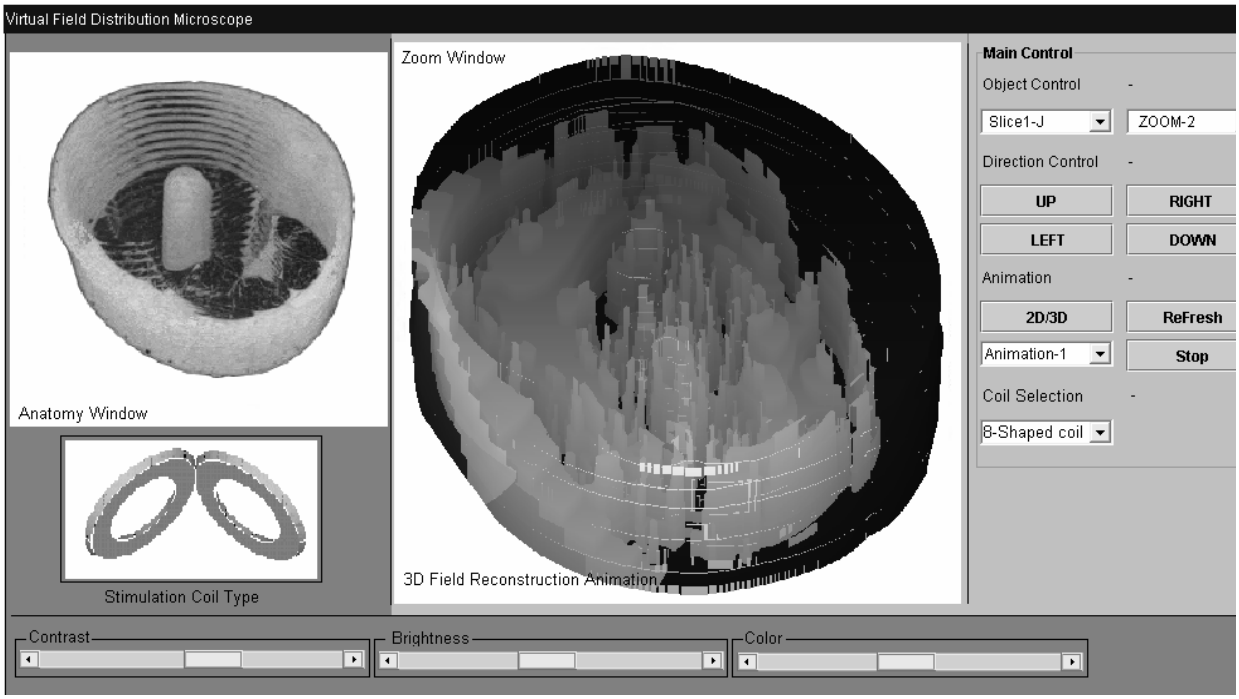


Figure 11. 3D Virtual microscope interface

VII. ARRAY SENSOR SYSTEM FOR MAGNETIC FIELD MEASUREMENT

For measurement of magnetic field in biological structures we developed measurement system using Anisotropic Magneto-Resistive (AMR) sensors. AMR sensors are based on anisotropic magnetoresistance effect. AMR sensors are combined in array probes in order to increase productivity of measurement process and improving the performance of probes applied for magnetic field measurements. Arrays of very small magnetic sensors can be used to detect very small magnetic fields with very high spatial resolution. Sensor array design depends largely upon the specific application. Arrays can include two- and three-axis sensors to measure vector fields. They are configured as extended one-dimensional arrays to survey a wide area in a single pass. Two-dimensional arrays of sensors can be left in place to survey an area without moving the array. The design of a two-dimensional array with 9 sensors is shown in Fig.12. Each sensor is a Wheatstone bridge. The bridges are connected in parallel with a common supply and ground. An example of a two-dimensional array of seven sensors is shown in Fig.13. This array can assure direct magnetic field image as well as field gradient in XZ plane. The total width of both arrays is 16 mm and the length is 22 mm. They are detecting the vertical component (Y) of the magnetic

field. Design of a two-dimensional array with 8 sensors is shown in Fig.14. This type of sensor can assure simultaneously information of two components of magnetic field flux density components (X-Y).

Several types for sensor signal pick up circuit systems are considered in Fig. 15-17.

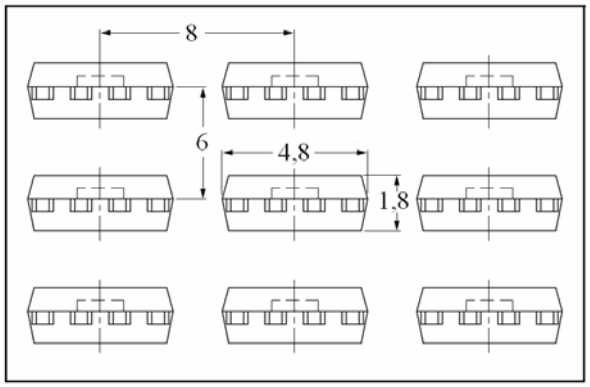


Fig.12. 3x3-element square array.

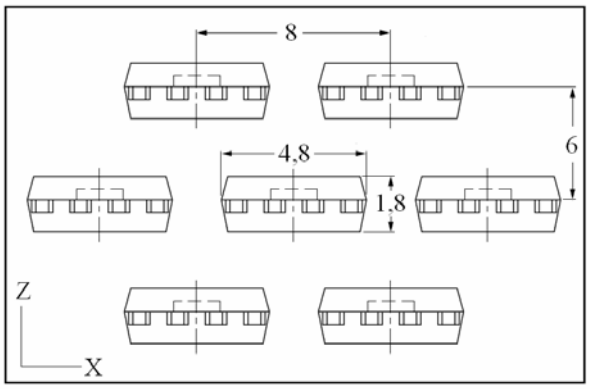


Fig.13. 7-element hexagonal array.

First array circuit in Fig.14 is based on National Instruments USB-6008 data acquisition device. Voltage range of USB-6008 is 10V at resolution 14,7mV with accuracy ±(1,7%)[20]. Limitation of this circuit is the number of analog input channels of data acquisition device.

Second array circuit in Fig.15 uses multiplexing IC controlled by a signal generator. Pick-up voltage signal is measured with Protek-506 Digital multimeter with voltage range 400mV at resolution 0,1mV with accuracy ±(1,5%) [21].

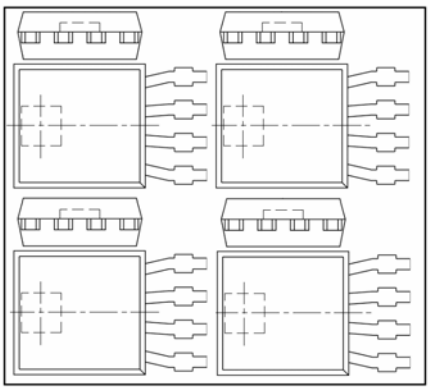


Figure 14. X-Y magnetic field flux density components array.

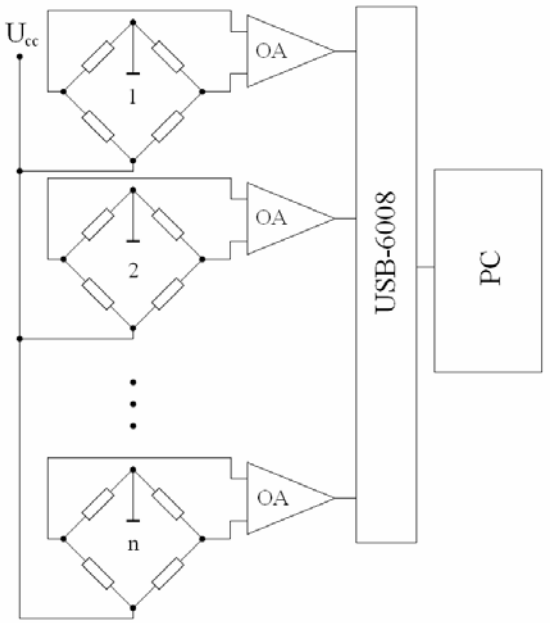


Fig.15. Signal pick-up circuit with USB-6008.

USB-6008 is directly connected to the PC and LabVIEW. Virtual instrument is created for signal processing and storage. Protek-506 uses RS-232 interface for data collection. [21]

Third array circuit in Fig.17 is a combination of both previously considered systems. It is uses multiplexing IC controlled by a signal generator and USB-6008 DAQ devise. Multiplexor IC unit controls the portions of data to USB-6008 DAQ devise. Maximal capacity of this circuit with 8ch.(multiplexor IC) × 8ch.(DAQ)=64ch. or 64 sensor elements.

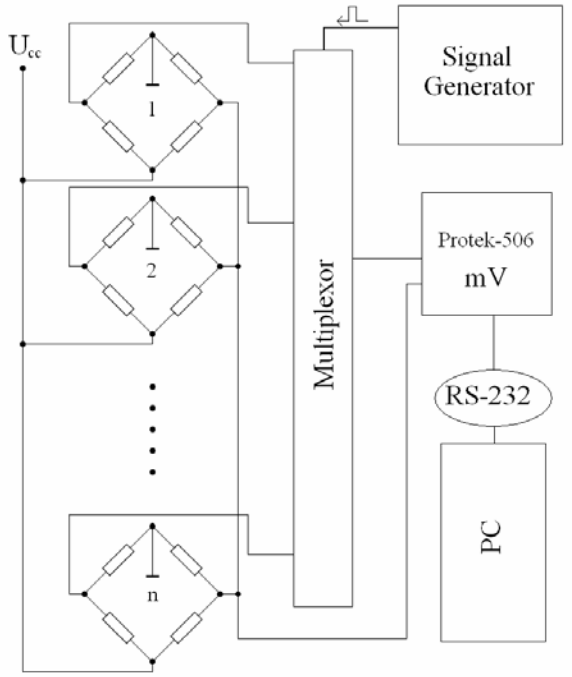


Fig.16. Signal pick-up circuit with Protek506.

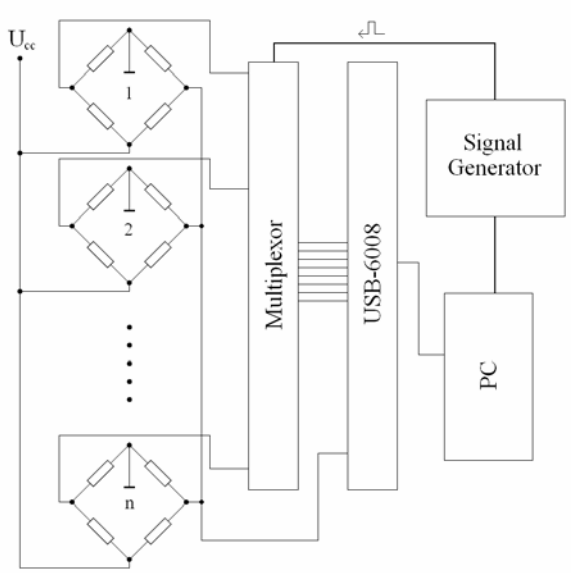


Figure17. Signal pick-up circuit.

Multiplexer in Fig. 17 activates eight pick-up AMR sensors at the time. The receiving configuration may be composed up to 64 sensor elements. Eight channels are activated in eight acquisition time intervals (or time slots of DAQ) to activate the complete probe in a very short period of time.

This multiplexing technique provides a large coverage in a single inspection pass while maintaining high scanning resolution.

VI. CONCLUSIONS

Computational model using FEM has been developed and used to investigate the electric and magnetic field distributions in human body produced by externally applied magnetic field. The model could use the CT images or cross-section images of the human biostructures.

Magnetic field and current distributions are visualized and analyzed. The 3D magnetic field visualization is realized by the 3D reconstruction approach using images of 2D magnetic field distribution. The 3D reconstruction approach combines new technologies of 3D visualizations and characterizes with flexibility, simplicity and portability. The proposed approach was successfully applied for 3D reconstruction and visualization of magnetic field as well as current distributions in the human leg exposed to externally applied time varying magnetic field.

The virtual microscope is developed for investigations of magnetic field distribution in biological structures during magnetic stimulation.

For measurement of magnetic field in biological structures we developed measurement system using anisotropic magneto-resistive sensors. The system give possibilities to measure weak magnetic field with high precisison and high spatial resolution.

Significant improvements in the efficacy and device performance used for medical diagnosis and therapy are expected as a result of a field analysis using numerical methods. In practical aspect this study can be used to build the effective methodologies for modeling, investigation of the fields, processes, phenomena in human body and for design of electromagnetic devices for medical therapy or diagnosis use.

VI. ACKNOWLEDGMENT

Parts of the research are supported by contract D002-157/2008 with Ministry of Science and Education.

REFERENCES

[1] I. Marinova, H. Endo, S. Hayano, and Y. Saito, "Image Reconstruction for Electromagnetic Field Visualization by an Inverse Problem Solution", *Int. Journal of Applied Electromagnetics and Mechanics*, 15 IOS Press, (2001/2002), pp. 403-408.

[2] I. Marinova, H. Endo, S. Hayano, and Y. Saito, "Inverse Electromagnetic Problems by Field Visualization", *IEEE Trans. Magn*. Vol. 40, No. 2, 2004, pp.1088-1093

[3] T. Doi, S. Hayano, I. Marinova, and Y. Saito, "Defect recognition in conductive materials by local magnetic field measurement", *Journal of Applied Physics*, Vol. 75, No. 10, 1994, pp. 5907-5909

[4] I. Marinova, C. Panchev, and D. Katsakos, "A Neural Network Inversion Approach for Electromagnetic Device Design", IEEE. Trans. Magn, Vol. 36, No. 4, 2000, pp. 1080-1084

[5] I. Marinova, C. Panchev, and D. Katsakos, "Gradient Coil Design for MRI by Neural Networks", The Joint Seminar'99, Nov. 1-3, Sapporo, Japan, 1999, pp.14-15

[6] C. Im, C. Lee, "Computer-Aided Performance Evaluation of a Multichanel Transcranial Magnetic Stimulation System", *IEEE Trans. Mag*n., Vol. 42, No. 12, 2006, pp. 3803-3808

[7] I. Marinova and L. Kovachev, "Inverse Approach for Determination of the Coils Location in Magnetic Stimulation", in Applied Electromagnetics. Proceedings of the 3rd JBMSAEM, Sept. 15-17, Ohrid, Macedonia, 2000, pp. 140-146

[8] V. Krasteva , S. Papazov and I. Daskalov, "Magnetic Stimulation for Non-homogeneous Biological Structures", *BioMed Eng OnLine*. 1: 3, http://www.biomedical-engineering-online.com/content/1/1/3, 2002

[9] P. Basser, "Focal Magnetic Stimulation of an Axon", IEEE Trans. Biomedical Engineering, Vol. 41, No. 6, 1994)

[10] S. Ueno, "Inverse Problem Aspects in the Field of Biomagnetic Applications", Non-Linear Electro- magnetic System. V. Kose and J. Sievert (Eds.) IOS Press, 1998

[11] R. Jalinous, "Guide to Magnetic Stimulation", Magstim Company Ltd., 1998

[12] M. A. Stuchly, "Applications of Time-varying Magnetic Fields in Medicine", *Critical Review in Biomedical Engineering*, Vol. 18, No. 2, 1990, pp. 89-124

[13] J. P. Reilly, "Peripheral Nerve Stimulation by Induced Electric Currents: Exposure to Time Varying Magnetic Fields", *Medical & Biological Engineering & Computing*, 1998, pp. 101-118

[14] I. Marinova and V. Mateev,"Virtual Magnetic Microscope", Proceedings of 16th symposium on Metrology and Metrology Assurance, Sept. 12-14, Sozopol, Bulgaria, 2006, pp. 138-142

[15] C. Smith, B. Schneider, A. Pohm. High-Resolution, Chip-Size Magnetic Sensor Arrays. Sensors Magazine, Vol. 20(3), 2003, pp. 44-49.

[16] B. Marchand, F. Vacher, C. Gilles-Pascaud, JM. Decitre, C. Fermon. High Resolution Eddy Current Probes For Non Destructive Testing. 34th Annual Review of Progress in Quantitative Nondestructive Evaluation. AIP Conference Proceedings, Vol. 9(75), 2008, pp. 313-320.

[17] Vacher, F., C. Gilles-Pascaud, J. M. Decitre, C. Fermon, M. Pannetier. Non Destructive Testing with GMR Magnetic Sensor Arrays. ECNDT, Vol. 4, 2006, pp. 13-18.

[18] Philips Semiconductors. KMZ10B Magnetic Field Sensor - Product Specification. 1998.

[19] Philips Semiconductors. Magnetic Field Sensors - General. 1998.

[20] National Instruments Corporation. USB-6008/6009 User Guide And Specifications. 2005.

[21] http://www.protektest.com.